Materials Sciences and Applications, 2022, 13, 317-333
https://www.scirp.org/journal/msa
ISSN Online: 2153-1188
ISSN Print: 2153-117X

Raman Spectroscopy Analysis of Wollastonite/Tricalcium Phosphate Glass-Ceramics after Implantation in Critical Bone Defect in Rats

Mauricio Mitsuo Monção[1,2*], Isabela Cerqueira Barreto[2], Fúlvio Borges Miguel[2], Luiz Fernando Cappa De Oliveira[3], Raul Garcia Carrodeguas[4], Roberto Paulo Correia De Araújo[5]

[1]Department of Technology in Health and Biology, Federal Institute of Education, Science and Technology of Bahia, Salvador, Brazil
[2]Laboratory of Tissue Bioengineering and Biomaterials, Federal University of Bahia, Salvador, Brazil
[3]Nucleus for Spectroscopy and Molecular Structure, Federal University of Juiz de Fora, Juiz de Fora, Brazil
[4]Noricum SL, San Sebastián de los Reyes, Madrid, Spain
[5]Institute of Health Sciences, Federal University of Bahia, Salvador, Brazil
Email: *maurimitsuo@yahoo.com.br

How to cite this paper: Monção, M.M., Barreto, I.C., Miguel, F.B., De Oliveira, L.F.C., Carrodeguas, R.G. and De Araújo, R.P.C. (2022) Raman Spectroscopy Analysis of Wollastonite/Tricalcium Phosphate Glass-Ceramics after Implantation in Critical Bone Defect in Rats. *Materials Sciences and Applications*, **13**, 317-333.
https://doi.org/10.4236/msa.2022.135017

Received: April 6, 2022
Accepted: May 16, 2022
Published: May 19, 2022

Abstract

In this work wollastonite/tricalcium phosphate (W/TCP) glass-ceramics with three W/TCP weight ratios (20/80; 60/40 and 80/20) were implanted in rat calvaria and the modifications taking place during implantation were studied by Raman spectroscopy. The experimental glass-ceramics were composed of different contents of βW, αW, βTCP, αTCP, and glassy phases. Materials were implanted for 7-, 15-, 45- and 120-day periods after which the implanted materials were recovered and analyzed by FT-Raman spectroscopy. The results suggested that the αW phase reabsorbs fast during implantation in the glass-ceramics 60/40 and 80/20, whereas βTCP and αTCP glass-ceramic are gradually attenuated and replaced by biological apatite-like bands. In the glass-ceramic 20/80, the bands related to the βTCP phase remained unvaried in all analyzed periods. New bands associated with the deposition of collagenous material appeared during implantation for all 60/40 and 80/20 glass-ceramics experimental groups, but important differences in intensities between both groups. The spectra corresponding to implants of 60/40 glass-ceramic at the 120-day period were very similar to those of the control group (normal cortical bone), with regards to Raman shifts and intensities, as well as in the FWHM value of the 962 cm^{-1} apatite band (ν_1 PO_4 in hydroxyapatite), evidencing that apatite deposited at the implant site has the same crystallinity than biological apatite in normal bone mineral. The

glass-ceramic 20/80 behaved just as an osteoconductive filling material, while glass-ceramics 60/40 and 80/20 were able to induce deposition of organic matrix mineralized new tissue. The 60/40 glass-ceramic showed the best performance and the most similar Raman spectrum to normal cortical bone.

Keywords

Raman Spectroscopy, Glass-Ceramics, Wollastonite, Tricalcium Phosphate

1. Introduction

The treatment of pathologic or traumatic extensive bone losses requires the application of bone substitutes since the natural physiological bone healing mechanism is insufficient to reach total bone tissue regeneration in a short time [1]. Currently, all the known materials used as bone substitutes still have some limitations and the search for the ideal bone substitute continues [2]. Several synthetic materials have been proposed for bone regeneration, among them, those consisting of several components that contribute with properties to render enhanced osteoinduction and osseointegration are attracting considerable attention [3].

Glass-ceramics belonging to the binary system wollastonite-tricalcium phosphate (W/TCP) has been extensively studied in the last two decades as they exhibit greater bioactivity and better mechanical resistance than the well-known calcium phosphate bioceramics [3]-[8]. The *in vitro* and *in vivo* bioactivity of W and its potential in bone regeneration have been well established in many published and explained on the basis of its incongruent dissolution and the calcium and silicon ions released when in contact with physiological fluids [9]. In particular, the silicon ion has a well-recognized capacity to induce osteogenesis and angiogenesis [9] [10].

Furthermore, the addition of W to calcium phosphates to manufacture sintered composites contributes to reinforcing and densifying the resulting glass-ceramic and improving its bioactivity [10].

Calcium phosphates are similar to the mineral phase of bone matrix, teeth, and calcified tissues. TCP is one of the most utilized calcium phosphates as bone substitute, due to its partial biodegradability, osteoconductivity and bone adhesion. Such properties result in its wide clinical use, as well as its application in the development of new composites with the purpose of bone regeneration [11] [12] [13].

Thus, combining the properties of W and TCP in the form of sintered glass-ceramic with different W/TCP ratios for the sake of increased osteoinduction and resorption may result in a bone substitute with better properties than its components. Moreover, the use of different W/TCP weight ratios may be a good strategy to tune the *in vivo* resorption rate of W/TCP glass-ceramics [14] [15]. The ideal amount of each component in the glass-ceramic becomes a chal-

lenge in the quest for the better performance of the material in the host organism, which is necessary to evaluate by *in vivo* implantation models.

Among the various techniques available, Raman spectroscopy has been widely used in the characterization of glasses and ceramics as well as in the assessment of *in vivo* responses to bone regeneration materials [16] [17] [18] [19]. It is a non-destructive technique requiring no or little preparation of samples and is widely used in molecular and structural analysis of complex compounds. This technique is based on the inelastic scattering of monochromatic light by the sample and the analysis of the frequency shift of the scattered light, which provides information about vibrational, rotational and other low-frequency transitions in molecules or crystals [20] [21] [22] [23].

In this scenario, this work studied the compositional modifications of W/TCP glass-ceramics with different W/TCP weight ratios after implantation in a critical bone defect model in rats for several periods, using Raman spectroscopy, and describes the ability of the studied glass-ceramics to induce the formation of organic matrix and mineralization of newly formed tissue, aiming to identify the best performance during the bone regeneration.

2. Materials and Methods

2.1. Glass-Ceramics

Experimental W/TCP glass-ceramics (W/TCP weight ratios: 80/20, 60/40 and 20/80) were kindly supplied by the Institute of Ceramics and Glass (ICV-CSIC, Madrid, Spain).

They were manufactured from powders of natural wollastonite, $CaSiO_3$ (NYCO, NYAD M1250, Batch Number M1404227J01) and tricalcium phosphate, $Ca_3(PO_4)_2$ (Sigma-Aldrich, Ref. 21218, Batch Number BCBM7330V). Briefly, the required amounts of both raw materials were mixed with isopropanol and the mixture was ball milled in an attrition mill. The resulting slurry was dried at 60˚C overnight and the dry cake was sintered at the selected temperature and dwelling time (20 - 80: 3 hr. at 1250˚C; 60 - 40: 1 hr. at 1250˚C; and 80 - 20 = 5 min. at 1250˚C). The sintered cakes were crushed in a jaw mill and sieved to collect particles with sizes in the range of 0.6 - 0.4 mm.

Granulate 60/40 was received sterile (25 kGy, e-beam) whereas 20/80 and 80/20 granulates were received non-sterile and sterilized by dry heat (180˚C, 30 min) prior to being used.

The 20 - 80 granules consisted mainly of crystalline β and αTCP and βW, in this order of abundance, and minor amounts of crystalline αW and amorphous glassy phase (AGP). On the other hand, 60/40 and 80/20 granules were composed of crystalline αW and βTCP and AGP. The chemical and phase compositions of the experimental materials are resumed in **Table 1**.

2.2. Animal Model and Implantation Procedure

The study was approved by the Ethics Committee on Animal Use of the Federal

Table 1. Chemical and phase compositions of the experimental glass-ceramics.

W-TCP Glass-ceramics	Oxides composition (wt.%)				Phase composition[a]				
	CaO	SiO_2	P_2O_5	Others[b]	αW	βW	βTCP	αTCP	AGP[c]
20/80	52.6	10.5	36.7	0.2	+	-	+++	++	-
60/40	49.2	31.5	18.4	0.9	++	nd[c]	++	nd	+++
80/20	47.6	42.1	9.2	1.1	++	nd	+	nd	+++

a. Semi-quantitative scale: +++ Most abundant phase; ++ Abundant; + Minor; - Scarce. b. Trace impurities as MgO, Al_2O_3, K_2O, Na_2O, Fe_2O_3, TiO_2. c. nd: non detected; AGP.: amorphous glassy phase.

University of Bahia, Brazil, (No. 128/2017), and followed the Guide for the Care and Use of Laboratory Animals prepared by the National Academy of Sciences [24], as well as the norms of the National Council for the Control of Animal Experimentation (CONCEA). Seventy-two adult male rats (Rattus norvegicus) weighing 350 - 400 g and 4 - 5-month age were used. Animals were kipped in individual cages at a temperature of 22˚C (±2) exposed to alternating periods of 12 hr. light and 12 hr. dark and fed and watered *ad libitum*. Animals were randomly distributed into experimental 4 groups (n = 20 each): three groups underwent surgery to create a circular bone defect of 8 mm in diameter in the central portion of the calvaria which was filled with one of the experimental glass-ceramics 20/80, 60/40, and 80/20. The fourth group (CG) did not undergo surgery and was used as a control to establish the spectroscopic parameters of the normal cortical bone of the calvaria.

Inside each group, subgroups (n = 5) were sacrificed after implantation periods of 7, 15, 45 and 120 days. The calvarias were removed, dissected, and fixed in 10% formaldehyde (v/v) at 4˚C - 8˚C. Fixed samples were then prepared according to Meade *et al.* [25], this is, were removed from the fixing solution, washed in filtered water, and immersed in 0.9% saline solution for ten minutes, then removed and dried with a paper towel. The experimental design is shown in **Figure 1**.

2.3. Raman Spectroscopic Analysis

An FT-Raman Spectrophotometer RFS 100/S (Bruker, Germany) with YAG: Nd laser (1064 nm) excitation source and Ge-diode, cooled at liquid N_2 temperature was used. The sample was directly positioned in the sample holder with the laser beam adjusted to a power of 10 mW and focused on the central portion.

Spectra in the region 300 - 3500 cm^{-1} were obtained with a resolution of 4 cm^{-1} and an accumulation of 512 scans. These parameters were obtained from previous experiments to obtain the maximum signal-to-noise ratio without altering the physical and chemical integrity of samples.

OPUS 6.0 software (Bruker, Germany) was used to acquire and process Raman data, and all spectra were obtained at least three times, after focusing the

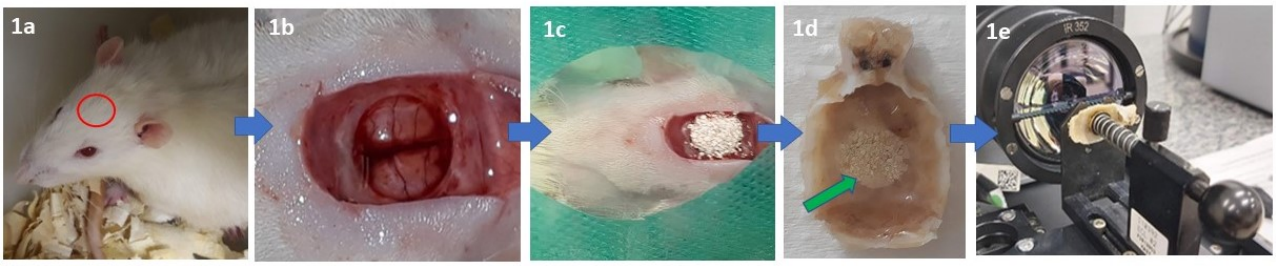

Figure 1. Experimental design: (a) Site were deffect surgery was practiced; (b) Aspect of the critical size bone defect (8 mm); (c) Deffect filled with experimental glass-ceramic; (d) Calvaria specimen with the implant site at the central portion (green arrow); and (e) Position of sample in the FT-Raman instrument.

laser beam at a different point on the sample, to verify the reproducibility of the system and possible uncertainties in intensity or Raman shift of the vibrational bands observed.

GRAMS/AI 7.02 software package (Thermo Galactic, USA) was used for import/export of Bruker OPUS File Format data and conversion to ASCII-XY. The spectra were plotted in OriginLab® version 2020b program, and analyzed for the presence, position, width, and intensities of the Raman bands. The spectra of the glass-ceramics, as received, and after the different implantation periods were analyzed to identify the modifications associated with resorption or permanence of the constituting crystalline phases, or the deposition of new organic or inorganic substances related to new bone tissue formation at the implant site. The assignation of the bands observed in the experimental spectra was carried out on the basis of the phase composition of the experimental glass-ceramics in **Table 1** and the data published in the literature [26]-[31].

3. Results

The spectra of the group 20/80 after the different periods of implantation is displayed in **Figure 2**. After 7, 15 and 45 days the characteristic Raman bands of αW, β- and αTCP phases were still distinguishable. Additionally, new bands arose at 1668, 1452 and 877 cm^{-1} with very weak intensities during implantation. At 120-day period, the characteristic bands of the βTCP phase remain but those corresponding to αW (580 and 374 cm^{-1}) are no longer observed [19] [27].

The results for the 60/40 and 80/20 experimental groups are shown in **Figure 3** and **Figure 4**, respectively. In these experimental groups bands at 1668 cm^{-1} (amide I); 1452 cm^{-1} (CH_2 and CH_3 lipids/collagen); 1271 and 1248 cm^{-1} (amide III); 1005 cm^{-1} (phenylalanine); 877, 856 and 818 cm^{-1} (proline, hydroxyproline and tyrosine), all consistent with the deposition of collagen on the implant site, were observed [32].

These groups also showed spectral modifications around 1071, 592 and 432 cm^{-1}, consisting of the appearance of bands with significant intensity differences between groups. From the 7-day period, the main bands attributed to the αW mineral phase (1076, 985, 580 and 374 cm^{-1}) [19] [26] [28] are no longer detected, suggesting that it is quickly resorbed in the physiological environment.

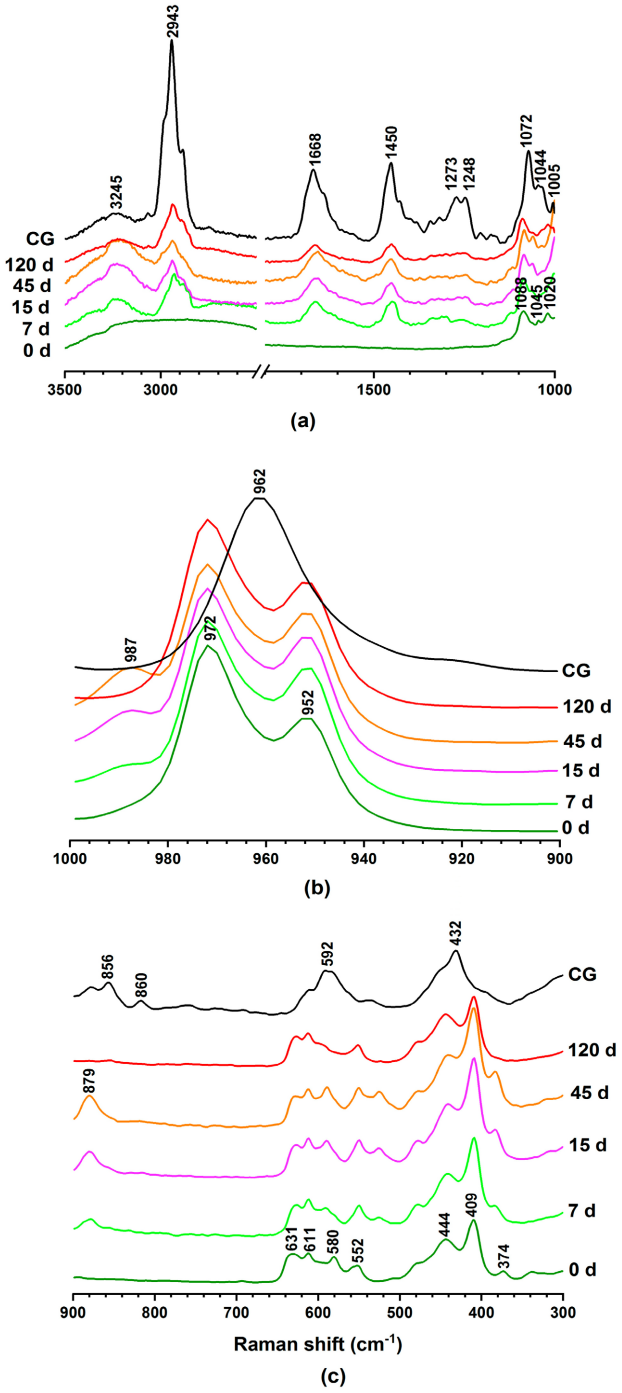

Figure 2. Raman spectra of 20/80 glass-ceramic: before (0 d) and after implantation for 7-, 15-, 45-, and 120-day periods, and the spectrum of non-implanted rat calvaria (CG). Wavenumber range (a) 3500 - 1000 cm^{-1}; (b) 1000 - 900 cm^{-1}; (c) 900 - 300 cm^{-1}.

On the other hand, the most prominent bands attributed to βTCP and αTCP phases (974 and 954 cm^{-1}, respectively) are observed up to the 45-day period. At 120-day period, 60/40 and 80/20 groups presented a unique band centered at 962 cm^{-1}. Only in the 80/20 group was visible a low intensity shoulder at 972 cm^{-1} due to a small amount of βTCP remaining [19] [29] [30] [31].

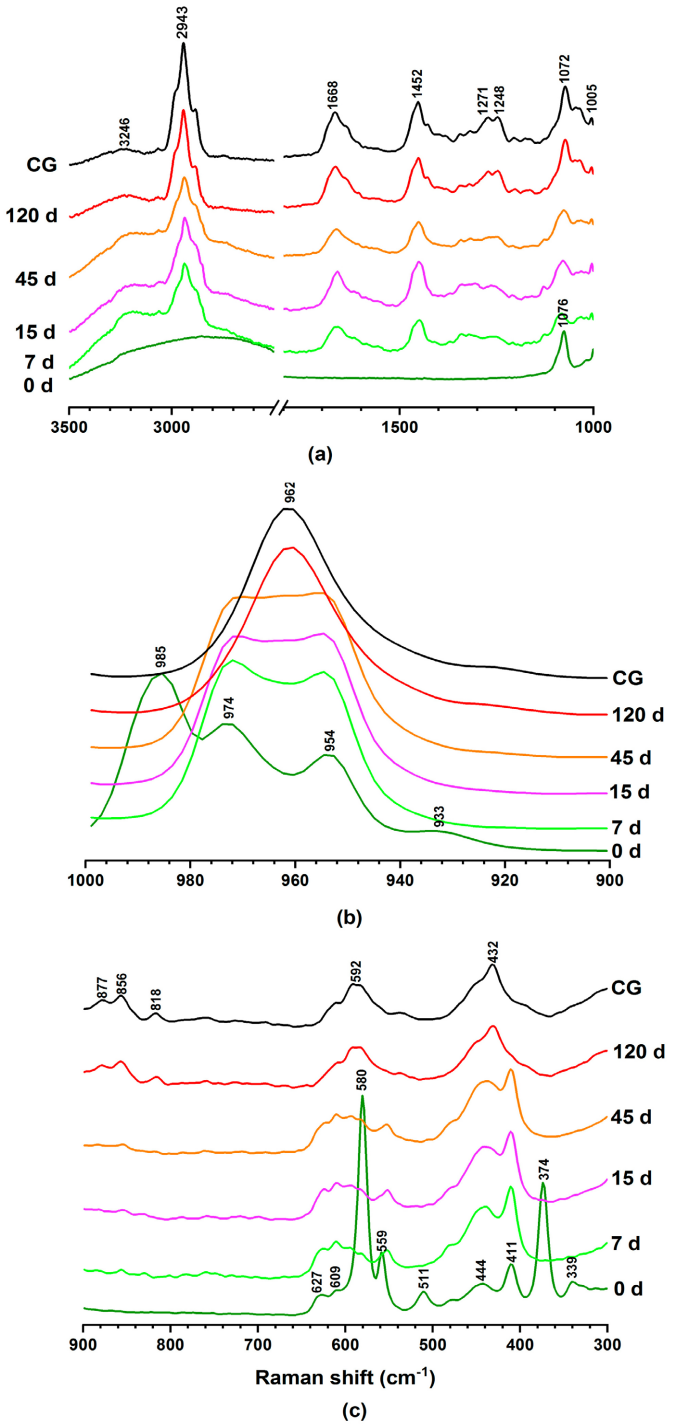

Figure 3. Raman spectra of 60/40 glass-ceramic: before (0 d) and after implantation for 7-, 15-, 45-, and 120 - day periods, and the spectrum of non-implanted rat calvaria (CG). Wavenumber range (a) 3500 - 1000 cm^{-1}; (b) 1000 - 900 cm^{-1}; (c) 900 - 300 cm^{-1}.

In the 20/80 group, after implantation for 120 days, only a few bands associated with the deposition of organic components at the implant site were observed, whereas the bands attributed to the inorganic constituents of the glass-ceramic remained.

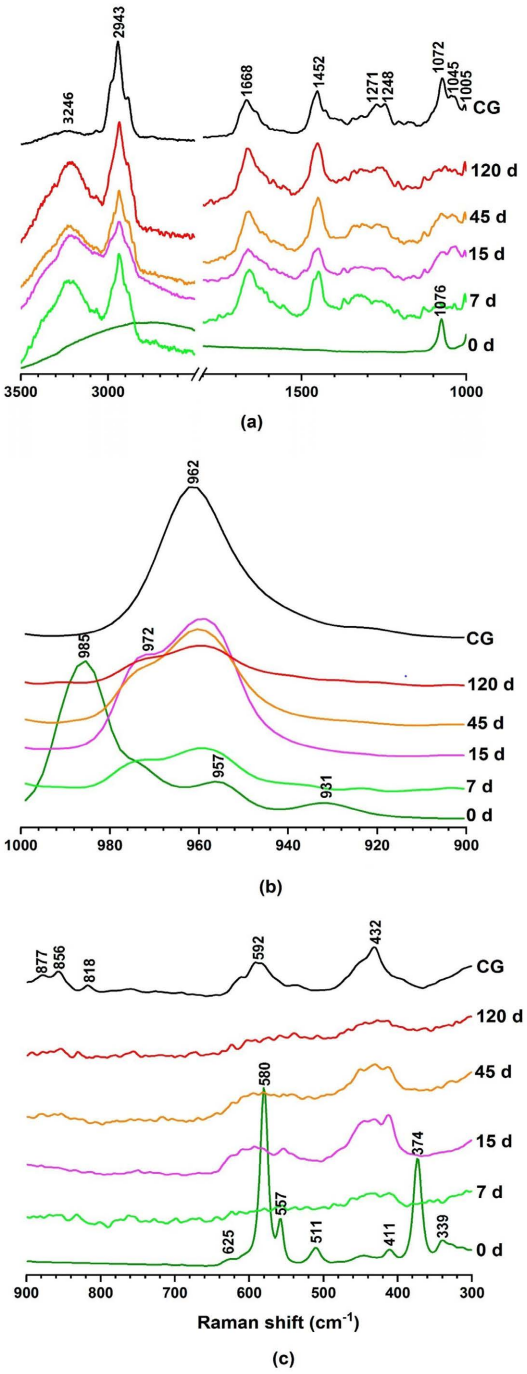

Figure 4. Raman spectra of 80/20 glass-ceramic: before (0 d) and after implantation for 7-, 15-, 45-, and 120-day periods, and the spectrum of non-implanted rat calvaria (CG). Wavenumber range (a) 3500 - 1000 cm^{-1}; (b) 1000 - 900 cm^{-1}; (c) 900 - 300 cm^{-1}.

Groups 60/40 and 80/20 presented bands very similar to Raman shifts, but with significant differences in their intensity ratios.

4. Discussion

The results of this study suggest that the experimental materials studied, *i.e.*,

W/TCP glass-ceramics with nominal weight ratios of 20/80, 60/40 and 80/20, exhibit quite different behavior with respect to resorption and new bone tissue deposition when implanted in rat calvaria.

The Raman vibrational profiles of the studied glass-ceramics experienced drastic modifications with the implantation time evidencing partial resorption of the inorganic constituents of the implanted material and the simultaneous deposition of organic and inorganic substances consistent with the formation of new bone tissue at the implant site.

The modifications in Raman shift, width and intensity of bands were dependent on the implantation period, and permit monitoring of the resorption of the different crystalline phases constituting the glass-ceramics as well as the deposition and formation of new substances both organic and inorganic.

Results indicated that the composition of 20/80 glass-ceramic remained almost unvaried up to the 45-day period; only after 120 days, the bands assigned to the *α*W disappeared. This suggests that the resorption rate of the 20/80 glass-ceramic is low and probably insufficient for bone regeneration purposes, keeping in mind that an ideal bone substitute should be resorbed and replaced by new bone tissue in a simultaneous and coordinated process [33]. However, results indicate that it can be used as an osteoconductive filling material for repairing bone defects.

Results indicated that the *α*W phase at the 7-day period of implantation of glass-ceramics was completely resorbed in groups 60/40 and 80/20, as evidenced by the absence of the characteristic bands at 1075, 985, 933, 580, 559 and 511 cm^{-1} [19] [26] [27] [28]. These results corroborate the results of previous studies that evaluated the behavior of ceramics containing *α*W and TCP, both *in vitro* and *in vivo* and reported its fast and incongruent dissolution and the pseudomorphic transformation of the TCP phase into biological apatite (Ap) [9].

Another study used wollastonite as bioactive, resorbable, and reinforcing filler in a W/polyvinyl alcohol composite for bone regeneration and concluded that it was possible to obtain controlled biodegradation and induce the formation of apatite on the material surface after 7 days of immersion in simulated body fluid [34]. Others also demonstrated that the presence of W in composites enhanced bioresorption rates and favored the initial bone repair dynamics [34] [35] [36] [37].

Considering the high *in vivo* resorption rate of *α*W it is reasonable to consider that different amounts of Ca and Si ions are released from the experimental materials used in this study which should be proportional to the *α*W content. The amount of surface amorphous silica and Ap nucleation on the implanted glass-ceramic should be dependent on its *α*W content as well [9] [38]. It is well known that calcium and silicon ions play an important in angiogenesis and osteogenesis *in vivo* [39] [40] [41].

Glass-ceramics with osteogenic behavior should primarily influence the local cell metabolism to promote cell differentiation into osteoblasts and stimulate their proliferation, with subsequent production of sufficient new bone tissue to

fill the critical bone defect. Maia Filho *et al.* [42] used Raman spectroscopy to study *in vivo* ceramic implants and found that those that induced the higher amounts of organic matrix deposition also achieved higher mineralization and new bone formation.

The results of the present study showed different spectral behavior for the formation of Raman bands around 1668 cm^{-1} (amide I), 1452 cm^{-1} (methyl group), 1271 and 1248 cm^{-1} (amide II), 1005 cm^{-1} (phenylalanine), 877, 856 and 818 cm^{-1} (proline, hydroxyproline and tyrosine) characteristic of collagen, as reported in studies that evaluated bone repair through Raman spectroscopy [43] [44] [45].

It is understood that the different percentage proportions of *α*W in glass-ceramics were decisive for the formation of organic components with extremes (20/80 and 80/20) exhibiting lower performances, and the 60/40 showing better performance, as resumed in **Figure 5**.

Although the literature does not define the ideal amount for silicon ion saturation and osteogenesis promotion, it is reasonable to infer that the amount of silicon ions released through *α*W resorption influences the osteogenesis potential of glass-ceramics under study.

Uribe *et al.* [46] investigated the *in vitro* osteogenic effects of dental follicle stem cells in simulated body fluid containing different Si concentrations and concluded that 25 μg/ml of Si had a significant positive effect on osteogenesis. On the other hand, solutions with Si < 25 μg/mL and >75 μg/mL did not show significant effects, whereas concentrations ≥ 100 μg/ml had an inhibitory effect on osteogenesis. Such findings corroborate the results of the present study, and permit to explain the lower deposition of organic matter on glass-ceramics with extreme contents of *α*W (20/80 and 80/20) and expect a poorer performance for bone regeneration as well.

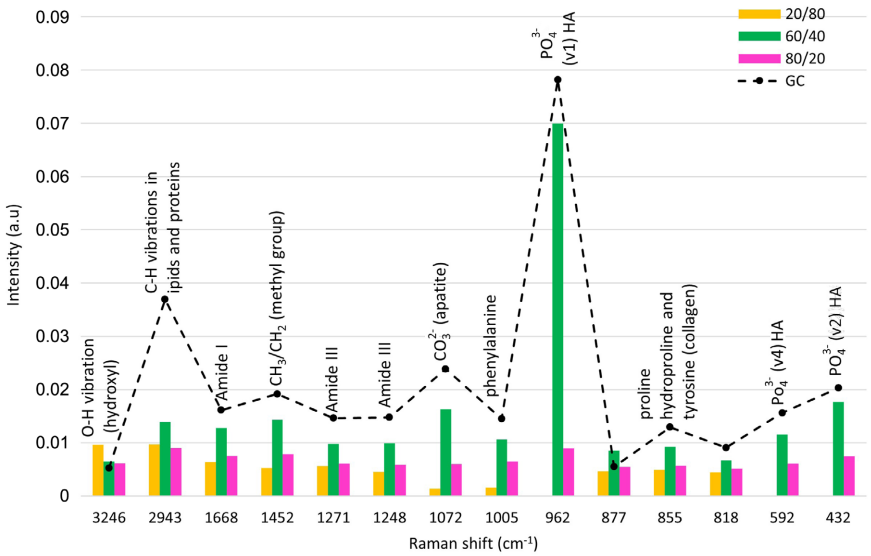

Figure 5. Raman band intensities reached by the experimental groups at 120 days after glass-ceramic implantation and comparison with CG.

However, dos Santos *et al.* [47] found better results for bone regeneration using a 3D scaffold made of glass-ceramic of W/TCP with a weight ratio of 20/80 evidencing that, besides chemical composition, biomaterial porosity (proportional to the material/body contact area) exerts a decisive influence on the interaction with the host organism.

The group 60/40 showed the formation of characteristic bands of organic components and achieved great spectral similarity with CG. In the present study, the positions, and intensities of bands such as those observed in CG indicate the formation and organization of new tissue with characteristics similar to the normal cortical bone [18].

Regarding the compositional modifications associated with mineral polymorphs, the spectral results of the group 20/80 group demonstrated the permanence of bands characteristic of the β- and α-TCP phases throughout all analyzed periods. This indicates that the 20/80 glass-ceramic performed as an osteoconductive filling material in the critical bone defect model. Groups 60/40 and 80/20 also presented bands attributed to β- and α-TCP phases (971 and 954 cm^{-1}, respectively), but only up to the 45-day period. After 120 days of implantation, only the 972 cm^{-1} band was visible in the 80/20 group as a shoulder of weak intensity, indicating a slower biodegradation rate of β- with regard to α-TCP. It is known that β-TCP and α-TCP mineral phases are isomorphs with the same chemical composition; however, their differences in crystal structures promote different *in vivo* behaviors [9]. Thus, the results found corroborate other studies that verified that the solubility index of the β-phase was lower than that of the αTCP phase resulting in longer permanence of βTCP at the implant site [48] [49] [50].

The results obtained also showed that in 60/40 and 80/20 groups, there were spectral changes consisting of the occurrence of new bands characteristics of vibrational modes of the PO_4 group. The Raman shifts observed (962, 592 and 432 cm^{-1}) are characteristic of the Ap composing bone mineral [32]; however, these bands presented important differences in intensities between the experimental groups.

The intensities of these bands can be directly related to the osteogenic potentials of the glass-ceramics under study. It is understood that, among several factors, the intensities of Raman bands are also related to the amount of active molecular species present in the sample [51]. Therefore, the intensity of bands exhibited at the implant site can be related to components formed and/or deposited over the evaluated periods.

The mineralization quality achieved in 60/40 and 80/20 groups was evaluated by comparing the values of Full Width at Half Maximum (FWHM) in cm^{-1} for the Raman band centered at 962 cm^{-1}, which is the more intense band in the Raman spectrum bone mineral phase, Ap. According to the literature, the FWHM value of this band is inversely related to the crystallinity degree of Ap [52]. In our study, the comparison of FWHM values of the 962 cm^{-1} band indicated different crystallinity degrees between experimental groups when compared to CG (see **Figure 6**).

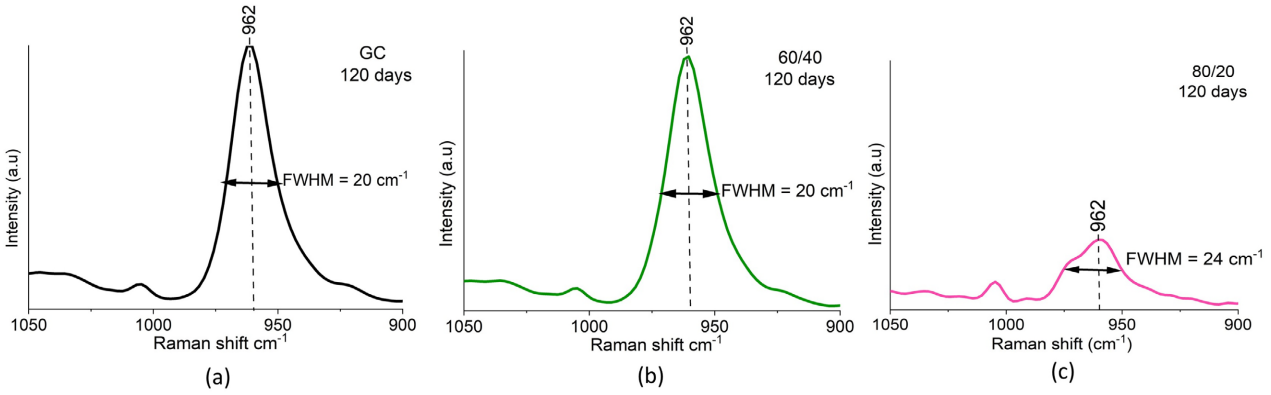

Figure 6. Comparison of FWHM of the 962 cm^{-1} band at 120 days after the implantation of glass-ceramics. (a) Control group; (b) 60/40 group; (c) 80/20 group.

The group 80/20 showed higher FWHM than the group 60/40 and CG. This indicates that 80/20 glass-ceramic induced the formation of poor crystalline Ap, probably because the fast dissolution of αW obtained lower performance for the formation of organic components and mineralization of the newly formed tissue, and 60/40 resulted in a greater amount and better organization of mineral components deposited and similarity to the spectrum of biological apatite in the CG.

Results of this study showed that the 60/40 glass-ceramic presented the greatest potential for future clinical applications as bone regeneration material.

5. Conclusion

The spectral changes observed for 60/40 and 80/20 glass-ceramics demonstrated that they exhibited gradual biodegradation and compositional changes during the *in vivo* implantation periods studied, indicating they have osteogenic potential, mainly the 60/40, which achieved the greater spectral similarity with normal bone. During the analysis periods, 20/80 glass-ceramic showed scarce spectral changes which evidence lower *in vivo* reactivity and resorption, and behavior typical of osteoconductive filling materials.

Acknowledgements

The authors would like to thank the Foundation for Research Support of the State of Bahia (FAPESB), the Department of Health Technology and Biology and the Laboratories of Materials Characterization, and of Radiological Physics of the Federal Institute of Education, Science and Technology of Bahia (IFBA) and express special thanks to Professor Fabiana Paim Rosa.

Raul Garcia Carrodeguas thanks grant PTQ-16-08573 funded by MICINN/AEI, Spain.

Conflicts of Interest

The authors declare no conflicts of interest regarding the publication of this paper.

References

[1] Sergi, R., Bellucci, D. and Cannillo, V. (2020) A Review of Bioactive Glass/Natural Polymer Composites: State of the Art. *Materials* (*Basel*), **13**, Article No. 5560. https://doi.org/10.3390/ma13235560

[2] Pereira, H.F., Cengiz, I.F., Silva, F.S., Reis, R.L. and Oliveira, J.M. (2020) Scaffolds and Coatings for Bone Regeneration. *Journal of Materials Science. Materials in Medicine*, **31**, 27. https://doi.org/10.1007/s10856-020-06364-y

[3] De Aza, P.N., Guitián, F. and De Aza, S. (1995) Phase Diagram of Wollastonite-Tricalcium Phosphate. *The Journal of the American Ceramic Society*, **78**, 1653-1656. https://doi.org/10.1111/j.1151-2916.1995.tb08865.x

[4] Magallanes-Perdomo, M., Luklinska, Z.B., Aza, A.H., Carrodeguas, R.G., Aza, S.D. and Pena, P. (2011) Bone-Like Forming Ability of Apatite-Wollastonite Glass Ceramic. *Journal of the European Ceramic Society*, **31**, 1549-1561. https://doi.org/10.1016/j.jeurceramsoc.2011.03.007

[5] Gaspar, A.M.M., Saska, S., Carrodeguas, R.G., De Aza, A.H., Pena, P., De Aza, P.N. and De Aza, S. (2008). Biological Response to Wollastonite Doped α-Tricalcium Phosphate Implants in Hard and Soft Tissues in Rats. *Key Engineering Materials*, **396-398**, 7-10. https://doi.org/10.4028/www.scientific.net/KEM.396-398.7

[6] Barbosa, W.T., De Almeida, K.V., De Lima, G.G., Rodriguez, M.A., Fook, M.V.L., Carrodeguas, R.G., Silva Junior, V.A., De Sousa Segundo, F.A. and De Sá, M.J.C. (2019) Synthesis and *in Vivo* Evaluation of a Scaffold Containing Wollastonite/β-TCP for Bone Repair in a Rabbit Tibial Defect Model. *Journal of Biomedical Materials Research Part B*: *Applied Biomaterials*, **108**, 1107-1116. https://doi.org/10.1002/jbm.b.34462

[7] Sola, D. and Grima, L. (2018) Laser Machining and *in Vitro* Assessment of Wollastonite-Tricacium Phosphate Eutectic Glasses and Glass-Ceramics. *Materials* (*Basel*), **11**, 125. https://doi.org/10.3390/ma11010125

[8] Ros-Tárraga, P., Mazón, P., Revilla-Nuin, B., Rabadán-Ros, R., De Aza, P.N. and Meseguer-Olmo, L. (2020) High Temperature $CaSiO_3$-$Ca_3(PO_4)_2$ Ceramic Promotes Osteogenic Differentiation in Adult Human Mesenchymal Stem Cells. *Materials Science and Engineering C*: *Materials for Biological Applications*, **107**, Article ID: 110355. https://doi.org/10.1016/j.msec.2019.110355

[9] García Carrodeguas, R. and De Aza, P.N. (2011) Main Contributions to Bioceramics by Salvador De Aza. *Boletín de la Sociedad Española de Cerámica y Vidrio*, **50**, 219-228. https://doi.org/10.3989/cyv.392011

[10] Wang, C., Xue, Y., Lin, K., Lu, J., Chang, J. and Sun, J. (2012) The Enhancement of Bone Regeneration by a Combination of Osteoconductivity and Osteostimulation Using β-$CaSiO_3$/β-$Ca_3(PO_4)_2$ Composite Bioceramics. *Acta Biomaterialia*, **8**, 350-360. https://doi.org/10.1016/j.actbio.2011.08.019

[11] Núñez-Rodríguez, L., Encinas-Romero, M., Gómez-Álvarez, A., Valenzuela-García, J. and Tiburcio Munive, G. (2018) Evaluation of Bioactive Properties of α and β Wollastonite Bioceramics Soaked in a Simulated Body Fluid. *Journal of Biomaterials and Nanobiotechnology*, **9**, 263-276. https://doi.org/10.4236/jbnb.2018.93015

[12] Jeong, J., Kim, J.H., Shim, J.H., Hwang, N.S. and Heo, C.Y. (2019) Bioactive Calcium Phosphate Materials and Applications in Bone Regeneration. *Biomaterials Research*, **9**, 23. https://doi.org/10.1186/s40824-018-0149-3

[13] Shim, K.S., Kim, H.J., Kim, S.E. and Park, K. (2018) Simple Surface Biofunctionalization of Biphasic Calcium Phosphates for Improving Osteogenic Activity and Bone Tissue Regeneration. *Journal of Industrial and Engineering Chemistry*, **68**, 220-228.

https://doi.org/10.1016/j.jiec.2018.07.048

[14] Safronova, T.V., Selezneva, I.I., Tikhonova, S.A., Kiselev, A.S., Davydova, G.A., Shatalova, T.B., Larionov, D.S. and Rau, J.V. (2020) Biocompatibility of Biphasic α, β-Tricalcium Phosphate Ceramics *in Vitro*. *Bioactive Materials*, **5**, 423-427. https://doi.org/10.1016/j.bioactmat.2020.03.007

[15] Domingues, J.A., Motisuke, M., Bertran, C.A., Hausen, M.A., Duek, E.A.R. and Camilli, J.A. (2017) Addition of Wollastonite Fibers to Calcium Phosphate Cement Increases Cell Viability and Stimulates Differentiation of Osteoblast-Like Cells. *The Scientific World Journal*, **2017**, Article ID: 5260106. https://doi.org/10.1155/2017/5260106

[16] De Souza, A.C., McNulty, C. Camilli, J., Bertran, C.A. and Motisuke, M. (2020) Calcium Phophate Cement Plus 10% Wollastonite Whiskers: An *in Vivo* Study. *Journal of Biomimetics*, *Biomaterials and Biomedical Engineering*, **47**, 117-126. https://doi.org/10.4028/www.scientific.net/JBBBE.47.117

[17] Fortaleza, L.M. de M., Alves, A.M.M., Maia Filho, A.L.M., Ferreira, D.C.L., Costa, C.L.S., Viana, V.G.F., Santos, J.Z.L.V., Oliveira, R.A, Viana, B.C., Gusmão, G.O.M. and Soares, L.E.S. (2020) Raman Spectroscopy Analysis of Bone Regeneration in a Rat Model by Implantation of a Biocompatible Membrane Scaffold with and without LED Photobiomodulation (λ 945 ± 20 nm). *Vibrational Spectroscopy*, **111**, Article ID: 103154. https://doi.org/10.1016/j.vibspec.2020.103154

[18] Timchenko, E.V., Timchenko, P.E., Pisareva, E.V., Vlasov, M. Yu., Volova, L.T., Fedorov, A.A., Fedorova, Ya.V., Tyumchenkova, A.S., Romanova, D.A., Daniel, M.A. and Subatovic, A.N. (2020) Optical Analysis of Bone Tissue by Raman Spectroscopy in Experimental Osteoporosis and Its Correction Using Allogeneic Hydroxyapatite. *Journal of Optical Technology*, **87**, 161-167. https://doi.org/10.1364/JOT.87.000161

[19] Mazón, P., Ros-Tárraga, P., Serena, S., Meseguer-Olmo, L. and De Aza, P.N. (2019) *In Vitro* Bioactivity and Cell Biocompatibility of a Hypereutectic Bioceramic. *Symmetry*, **11**, 355. https://doi.org/10.3390/sym11030355

[20] Borkowski, L., Sroka-Bartnicka, A., Polkowska, I., Pawlowska, M., Palka, K., Zieba, E., Slosarczyk, A., Jozwiak, K. and Ginalska, G. (2017) New Approach in Evaluation of Ceramic-Polymer Composite Bioactivity and Biocompatibility. *Analytical and Bioanalytical Chemistry*, **409**, 5747-5755. https://doi.org/10.1007/s00216-017-0518-0

[21] Ember, K.J.I., Hoeve, M.A., McAughtrie, S.L., Bergholt, M.S., Dwyer, B.J., Stevens, M.M., Faulds, K., Forbes, S.J. and Campbell, C.J. (2017) Raman Spectroscopy and Regenerative Medicine: A Review. *NPJ Regenerative Medicine*, **2**, 12. https://doi.org/10.1038/s41536-017-0014-3

[22] Das, R. and Agrawal, Y. (2011) Raman Spectroscopy: Recent Advancements, Techniques and Applications. *Vibrational Spectroscopy*, **57**, 163-176. https://doi.org/10.1016/j.vibspec.2011.08.003

[23] Butler, H.J., Ashton, L., Bird, B., Cinque, G., Curtis, K., Dorney, J., *et al.* (2016) Using Raman Spectroscopy to Characterize Biological Materials. *Nature Protocols*, **11**, 664-687. https://doi.org/10.1038/nprot.2016.036

[24] National Research Council (2011) Guide for the Care and Use of Laboratory Animals. 8th Edition, The National Academies Press, Washington DC.

[25] Meade, A., Clarke, C., Draux, F., Sockalingusm,G., Manfait, M., Lyng, F. and Byrne, H.J. (2010) Studies of Chemical Fixation Effects in Human Cell Lines Using Raman Microspectroscopy. *Analytical and Bioanalytical Chemistry*, **396**, 1781-1791.

https://doi.org/10.1007/s00216-009-3411-7

[26] Huang, E., Chen, C.H., Huang, T., Lin, E.H. and Xu, J.-A. (2000) Raman Spectroscopic Characteristics of Mg-Fe-Ca Pyroxenes. *American Mineralogist*, **85**, 473-479. https://doi.org/10.2138/am-2000-0408

[27] Swamy, V., Dubrovinsky, L.S. and Tutti, F. (2010) High-Temperature Raman Spectra and Thermal Expansion of Wollastonite. *Journal of the American Ceramics Society*, **8**, 2237-2247. https://doi.org/10.1111/j.1151-2916.1997.tb03113.x

[28] Richet, P., Mysen, B.O. and Ingrin, J. (1998) High-Temperature X-Ray Diffraction and Raman Spectroscopy of Diopside and Pseudowollastonite. *Physics and Chemistry of Minerals*, **25**, 401-414. https://doi.org/10.1007/s002690050130

[29] Jillavenkatesa, A. and Condrate, R.A. (1998) The Infrared and Raman Spectra of β-and α-Tricalcium Phosphate ($Ca_3(PO_4)_2$). *Spectroscopy Letters*, **31**, 1619-1634. https://doi.org/10.1080/00387019808007439

[30] De Aza, P.N., Santos, C., Pazo, A., De Aza, S., Cuscó, R. and Artús, L. (1997) Vibrational Properties of Calcium Phosphate Compounds. 1. Raman Spectrum of β-Tricalcium Phosphate. *Chemistry of Materials*, **9**, 912-915. https://doi.org/10.1021/cm960425d

[31] De Aza, P.N., Santos, C., Pazo, A., De Aza, S., Cuscó, R. and Artús, L. (1997) Vibrational Properties of Calcium Phosphate Compounds. 2. Comparison between Hydroxyapatite and β-Tricalcium Phosphate. *Chemistry of Materials*, **9**, 916-922. https://doi.org/10.1021/cm9604266

[32] Movasaghi, Z., Rehman, S. and Rehman, I.U. (2007) Raman Spectroscopy of Biological Tissues. *Applied Spectroscopy Reviews*, **42**, 493-541. https://doi.org/10.1080/05704920701551530

[33] Janicki, P. and Schmidmaier, G. (2011) What Should Be the Characteristics of the Ideal Bone Graft Substitute? Combining Scaffolds with Growth Factors and/or Stem Cells. *Injury*, **42**, 77-81. https://doi.org/10.1016/j.injury.2011.06.014

[34] Adams, L.A., Essien, E.R. and Kaufmann, E.E. (2019) Mechanical and Bioactivity Assessment of Wollastonite/PVA Composite Synthesized from Bentonite Clay. *Cerâmica*, **65**, 246-251. https://doi.org/10.1590/0366-69132019653742584

[35] Sharma, S., Patil, D.J., Soni, V.P., Sarkate, L.B., Khandekar, G.S. and Bellare, J.R. (2009) Bone Healing Performance of Electrophoretically Deposited Apatite-Wollastonite/Chitosan Coating on Titanium Implants in Rabbit Tibiae. *Journal of Tissue Engineering and Regenerative Medicine*, **3**, 501-511. https://doi.org/10.1002/term.186

[36] Xu, S., Lin, K., Wang, Z., Chang, J., Wang, L., Lu, J. and Ning, C. (2008) Reconstruction of Calvarial Defect of Rabbits Using Porous Calcium Silicate Bioactive Ceramics. *Biomaterials*, **29**, 2588-2596. https://doi.org/10.1016/j.biomaterials.2008.03.013

[37] Sun, M., Liu, A., Shao, H., Yang, X., Ma, C., Yan, S., Liu, Y., He, Y. and Gou, Z. (2016) Systematical Evaluation of Mechanically Strong 3D Printed Diluted magnesium Doping Wollastonite Scaffolds on Osteogenic Capacity in Rabbit Calvarial Defects. *Scientific Reports*, **6**, Article No. 34029. https://doi.org/10.1038/srep34029

[38] Guo, H., Wei, J., Song, W., Zhang, S., Yan, Y., Liu, C. and Xiao, T. (2012) Wollastonite Nanofiber-Doped Self-Setting Calcium Phosphate Bioactive Cement for Bone Tissue Regeneration. *International Journal of Nanomedicine*, **7**, 3613-3624. https://doi.org/10.2147/IJN.S32061

[39] Paluszkiewicz, C., Blażewicz, M., Podporska, J. and Gumuła, T. (2020) Nucleation of Hydroxyapatite Layer on Wollastonite Material Surface: FTIR Studies. *Vibra-*

tional Spectroscopy, **48**, 263-268. https://doi.org/10.1016/j.vibspec.2008.02.020

[40] Meseguer-Olmo, L., Aznar-Cervantes, S., Mazón, P. and De Aza, P.N. (2012) "*In Vitro*" Behaviour of Adult Mesenchymal Stem Cells of Human Bone Marrow Origin Seeded on a Novel Bioactive Ceramics in the Ca_2SiO_4-$Ca_3(PO_4)_2$ System. *Journal of Materials Science*: *Materials in Medicine*, **23**, 3003-3014. https://doi.org/10.1007/s10856-012-4742-z

[41] Chang, N.J., Chen, Y.W., Shieh, D.E., Fang, H.Y. and Shie, M.Y. (2015) The Effects of Injectable Calcium Silicate-Based Composites with the Chinese Herb on an Osteogenic Accelerator *in Vitro*. *Biomedical Materials*, **10**, Article ID: 055004. https://doi.org/10.1088/1748-6041/10/5/055004

[42] Maia Filho, A.l.M., Amaral, F.P.M., Martin, A.A. and Soares, L.E.S. (2014) Evaluation of Inorganic and Organic Bone Components after Application of an Apatite-Coated Al_2O_3 Implants as Scaffolds for Bone Repair. *Brazilian Archives of Biology and Technology*, **57**, 334-339. https://doi.org/10.1590/S1516-89132014005000002

[43] Omar, O., Engstrand, T., Kihlström B., Linder, L., Åberg, J., Shah, F.A., *et al.* (2020) *In Situ* Bone Regeneration of Large Cranial Defects Using Synthetic Ceramic Implants with a Tailored Composition and Design. *Proceedings of the National Academy of Sciences*, **117**, 26660-26671. https://doi.org/10.1073/pnas.2007635117

[44] Pinheiro, A.L.B., Soares, L.G.P., Marques, A.M.C., Cangussú, M.C.T., Pacheco, M.T.T. and Silveira, L.Jr. (2017) Biochemical Changes on the Repair of Surgical Bone Defects Grafted with Biphasic Synthetic Micro-Granular HA + β-Tricalcium Phosphate Induced by Laser and LED Phototherapies and Assessed by Raman Spectroscopy. *Lasers in Medical Science*, **32**, 663-672. https://doi.org/10.1007/s10103-017-2165-2

[45] Ozaki, H., Hamai, R., Shiwaku, Y., Sakai, S., Tsuchiya, K. and Suzuki, O. (2021) Mutual Chemical Effect of Autograft and Octacalcium Phosphate Implantation on Enhancing Intramembranous Bone Regeneration. *Science and Technology of Advanced Materials*, **22**, 345-362. https://doi.org/10.1080/14686996.2021.1916378

[46] Uribe, P., Johansson, A., Jugdaohsingh, R., Powell, J.J., Magnusson, C., Davila, M., *et al.* (2007) Soluble Silica Stimulates Osteogenic Differentiation and Gap Junction Communication in Human Dental Follicle Cells. *Scientific Reports*, **10**, Article No. 9923. https://doi.org/10.1038/s41598-020-66939-1

[47] dos Santos, G.G., Borges Miguel, I.R.J., Barbosa Junior, A.A., Barbosa, W.T., Almeida, K.V., García-Carrodeguas, R., Fook, M.V.L., Rodríguez, M.A., Borges Miguel, F., de Araújo, R.P.C. and Rosa, F.P. (2021) Bone Regeneration Using Wollastonite/β-TCP Scaffolds Implants in Critical Bone Defect in Rat Calvaria. *Biomedical Physicas & Engineering Express*, **7**, Article ID: 055015. https://doi.org/10.1088/2057-1976/ac1878

[48] Li, Y., Weng, W. and Tam, K.C. (2007) Novel Highly Biodegradable Biphasic Tricalcium Phosphates Composed of Alpha-Tricalcium Phosphate and Beta-Tricalcium Phosphate. *Acta Biomaterialia*, **3**, 251-254. https://doi.org/10.1016/j.actbio.2006.07.003

[49] Xie, L., Yu, H., Deng, Y., Yang, W., Liao, L. and Long, Q. (2016) Preparation, Characterization and *in Vitro* Dissolution Behavior of Porous Biphasic α/β-Tricalcium Phosphate Bioceramics. *Materials Science and Engineering*: *C*, **59**, 1007-1015. https://doi.org/10.1016/j.msec.2015.11.040

[50] De Aza, P.N., Peña, J.I., Luklinska, Z.B., and Meseguer-Olmo, L. (2014) Bioeutectic® Ceramics for Biomedical Application Obtained by Laser Floating Zone Method. *In*

Vivo Evaluation. Materials, **7**, 2395-2410. https://doi.org/10.3390/ma7042395

[51] Pelletier, M.J. (2003) Quantitative Analysis Using Raman Spectrometry. *Applied Spectroscopy*, **57**, 20A-42A. https://doi.org/10.1366/000370203321165133

[52] Karan, K., Yao, X., Xu, C. and Wang, Y. (2009) Chemical Profile of the Dentin Substrate in Non-Carious Cervical Lesions. *Dental Materials*, **25**, 1205-1212. https://doi.org/10.1016/j.dental.2009.04.006